Helium-oxygen ventilation in the presence of expiratory flow-limitation: a model study

Chiara Brighenti[1], Paolo Barbini[2], Gianni Gnudi[1], Gabriele Cevenini[2], Matteo Pecchiari[3], and Edgardo D'Angelo[3*]

[1]Dipartimento di Elettronica, Informatica e Sistemistica, Università di Bologna, 47023 Cesena, Italy, [2]Dipartimento di Chirurgia e Bioingegneria Università di Siena, 5310 Siena, Italy [3]Istituto di Fisiologia Umana I, Università degli Studi di Milano, 20133 Milan, Italy.

DOI: http://dx.doi.org/10.1016/j.resp.2006.12.012

*Corresponding author: Tel. +39-02-50315440; Fax +39-02-50315430
E-mail edgardo.dangelo@unimi.it

Abstract

A comparison between air and heliox (80% helium-20% oxygen) ventilation was performed using a mathematical, non-linear dynamic, morphometric model of the respiratory system. Different obstructive conditions, all causing expiratory flow limitation (EFL), were simulated during mechanical ventilation to evaluate and interpret the effects of heliox on tidal EFL and dynamic hyperinflation. Relative to air ventilation, intrinsic positive end-expiratory pressure did not change with heliox if the obstruction was limited to the peripheral airways, i.e. beyond the 7^{th} generation. When central airways were also involved, heliox reduced dynamic hyperinflation (DH) if the flow-limiting segment remained in the 4^{th} to 7^{th} airway generation during the whole expiration, but produced only minor effects if, depending on the contribution of peripheral to total apparent airway resistance, the flow-limiting segment moved eventually to the peripheral airways. In no case did heliox abolish EFL occurring with air ventilation, indicating that any increase in driving pressure would be without effect on DH. Hence, to the extent that chronic obstructive pulmonary disease (COPD) affects primarily the peripheral airways, and causes EFL through the same mechanisms operating in the model, heliox administration should not be expected to appreciably reduce DH in the majority of COPD patients who are flow-limited at rest.

Key words: chronic obstructive pulmonary disease, dynamic hyperinflation, flow-volume curve, airway collapsibility, mathematical model

1. Introduction

The use of helium-oxygen mixtures, usually 20% oxygen and 80% helium (heliox), was first introduced by Barach (1935) for the treatment of patients with obstructive pulmonary disease, based on the fact that in the presence of turbulent flow, the frictional pressure losses, and hence pipe resistance, decrease as gas density decreases. However, contrasting results concerning the effects of heliox administration on lung mechanics in obstructed patients have been reported by numerous studies (Grapé et al, 1960; Swidwa et al, 1985; Wouters et al, 1992; Jaber et al, 2000; Diehl et al, 2003; Gainnier et al, 2003; Jolliet et al, 2003; Palange et al, 2004; Pecchiari et al, 2004; Lee et al, 2005) and reviews (Manthous et al, 1997; Marini, 2000; Chevrolet, 2001; Rodrigo et al, 2002; Ho, 2003). This, together with the relatively high costs and technical difficulties of administration, points to the need of further evaluation of the effectiveness of heliox, particularly in patients with chronic obstructive pulmonary disease (COPD).

Because of the complexity of lung mechanics and the difficulty to gain knowledge of all the relevant variables and parameters, a comprehensive interpretation of the contrasting results of clinical investigations is difficult, and modelling can represent an alternative approach. An analysis of the effects of heliox was performed using a single-pipe model for the tracheobronchial tree (Papamoschou, 1995), the results supporting the beneficial effects of heliox. Because of its extreme simplicity, this model, which represented the tracheobronchial tree as a rigid pipe, could not account for several phenomena that occur in the real lung: of paramount importance, expiratory flow limitation (EFL), which often occurs in COPD patients (West,1998).

A mathematical model incorporating the main non-linear mechanical characteristics of the tracheobronchial tree was recently proposed to reproduce phenomena such as dynamic hyperinflation, intrinsic positive end-expiratory pressure, and tidal EFL (Barbini et al, 2005). In the present study, an improved version of this model has been used to simulate the response to heliox administration of patients with various, well defined mechanical alterations of the tracheobronchial tree, with the aim to assess the conditions under which this therapeutic intervention is beneficial, as well as the parameter that must be taken as a measure of this benefit. In the absence of flow limitation and independently of the level of airway resistance, the improvement of the breathing effort is limited to those circumstances in which appreciable turbulence develops and it is easily predictable. Thus, the model has been only used to simulate the conditions of patients with tidal EFL at rest, when the main beneficial effect of heliox administration is given by the fall of the end-expiratory lung volume, i.e. reduction of hyperinflation. Although for simplicity, the model simulates the conditions of a paralysed, intubated, mechanically ventilated subject, this does not limit the generalisation of the results, since they are obtained in the presence of EFL.

2. Methods

A mathematical, non-linear dynamic, morphometric model (Barbini et al, 2005), that includes both the wave speed and viscous mechanism limiting expiratory flow (Hyatt, 1983), was used to simulate the respiratory mechanics of patients undergoing mechanical ventilation with air or heliox at constant inflation flow and fixed tidal volume (V_T=0.6 l), respiratory rate (15 min^{-1}), and duty cycle (0.25). During air breathing, the following equations were used to account for the flow (q, $l \cdot s^{-1}$) dependence of the endotracheal tube (Mallinckrodt® #8) and expiratory valve resistance ($cmH_2O \cdot s \cdot l^{-1}$) during ventilation with air: $0.52+4.32q$ and $0.35+8.7q$, respectively (Barbini et al, 2005). With heliox ventilation, the constants accounting for the turbulent flow component were reduced by 40% (Gerbeaux et al, 2005).

The morphometry of the model's tracheobronchial tree was derived from Weibel's symmetrical representation (Weibel, 1963). Each branch of the conductive zone was represented as a cylinder of constant length, the diameter of which varies with transmural pressure. Three parameters, accounting for airflow resistance, air inertance and airway wall compliance, characterized every branch of generation n.

The branch resistance was described as a non-linear resistor

$$R_{b_n} = \frac{128 \eta l_{b_n}}{\pi d_{b_n}^4} \cdot \left(1 + k_{b_n} \left| q_{b_n} \right|\right) \tag{1}$$

where η is the viscosity of the gas mixture, k_{b_n} is a branch constant depending on the density of the gas mixture, and l_{b_n}, d_{b_n} and q_{b_n} are branch length, diameter and gas flow, respectively. Two gas mixtures were considered: standard air and heliox, with density 1.12 and 0.37 $kg \cdot m^{-3}$ and viscosity 189 and 209 micropoise, respectively. In each airway generation, the parameter k_{b_n} was estimated for both gas mixtures in a flow range between 10 and 60 $l \cdot min^{-1}$, using resistance data from Pedley et al. (1970).

Branch inertance was represented conventionally as a function of gas mixture density (ρ) and branch length and diameter

$$L_{b_n} = \frac{4 \cdot \rho \cdot l_{b_n}}{\pi \cdot d_{b_n}^2} \tag{2}$$

Branch compliance was obtained as the derivative of branch volume (V_{b_n}) with respect to transmural pressure (P_n)

$$C_{b_n} = \frac{\mathrm{d}V_{b_n}}{\mathrm{d}P_n} \tag{3}$$

where branch volume is calculated on the basis of the actual branch diameter and length.

The branch diameter of generation n expressed as a percentage of its maximum value (d_{b_n}%) is a function of transmural pressure (Lambert, 1989)

$$d_{b_n}\% = \begin{cases} 100 \cdot \left(\alpha_{0_n} \cdot \left(1 - \dfrac{\alpha'_{0_n} \cdot P_n}{\alpha_{0_n}} \right)^{-1} \right)^{0.5}, & P_n < 0 \\ 100 \cdot \left(1 - (1-\alpha_{0_n}) \cdot \left(1 - \dfrac{\alpha'_{0_n} \cdot P_n}{(\alpha_{0_n} - 1) \cdot g_n} \right)^{-g_n} \right)^{0.5}, & P_n \geq 0 \end{cases}$$

$$\alpha_{0_n} = \left(A_{b_n} / A_{b_n \max} \right)\Big|_{P_n=0}; \quad \alpha'_{0_n} = \left(d\alpha_n / dP_n \right)\Big|_{P_n=0} \tag{4}$$

where A_{bn} and $A_{bn\,\max}$ are the branch area of generation n and its maximum value, respectively, and $\alpha_n = A_{bn}/A_{bn\,\max}$. The three parameters ($\alpha_{0n}$, α'_{0n}, g_n) that define the d_{b_n}%─P_n curve, are reported in Table 1 for the normal tracheobronchial tree.

Because of regular branching dichotomy, all the 2^n airways in the n^{th} generation were replaced with a single airway having resistance, inertance and compliance given by $R_n = R_{b_n}/2^n$, $L_n = L_{b_n}/2^n$, and $C_n = 2^n \cdot C_{b_n}$. The airflow entering the n^{th} generation is therefore $q_n = 2^n \cdot q_{b_n}$ and the transmural pressure of the n^{th} generation is equal to branch transmural pressure P_n.

The pressure drop at the junction between two generations was described by the Bernoulli equation, assuming that the transition from one generation to the next takes place over such a short distance that friction losses can be considered negligible and that there is no pressure recovery when the gas mixture goes into a generation with a larger total cross-sectional area (Barbini et al, 2005). Thus the total pressure drop across the n^{th} generation is:

$$P_{n-1} - P_n = \frac{1}{2}\, \xi\, \rho \left(\frac{q_n^2}{A_n^2} - \frac{q_{n-1}^2}{A_{n-1}^2} \right) + R_n\, q_n + \frac{d(L_n q_n)}{dt} \tag{6}$$

where A_n is the total cross-sectional area of the n^{th} generation and ξ is a coefficient set equal to 1 when the gas flow enters a generation with a smaller total cross-sectional area and equal to 0 in the reverse condition.

Finally, the respiratory zone was modeled as a parallel combination of a spring and dashpot with elastance and resistance of 12 $cmH_2O \cdot l^{-1}$ and 0.5 $cmH_2O \cdot s \cdot l^{-1}$, respectively, while the elastance of the chest wall was set at 10 $cmH_2O \cdot l^{-1}$.

The present model of lung mechanics depicts a non-linear dynamic system which cannot be solved analytically; only numerical solutions are feasible. The model was, therefore, implemented in MATLAB-SIMULINK, using a variable-step solver for stiff problems, and cycled until a steady end-expiratory lung volume is reached. The difference between this and the static equilibrium volume of the respiratory system, arbitrarily set to zero, was taken as a measure of dynamic hyperinflation and indicated as ΔFRC, while the corresponding intrinsic positive end-expiratory pressure (PEEPi) was given by the alveolar pressure at end-expiration.

In order to increase airway collapsibility leading to tidal EFL, the d_b%─P curve of the selected generations was modified as follows: maximum d_b was reduced to a fixed 85% of the normal value, while the d_b%─P curves were shifted rightwards to variable extents. In all cases, the resistance of the respiratory zone was increased four folds. As shown in Fig. 1, four types of alterations of the bronchial tree were simulated:

Case A: moderate (generations 8 to 11) to marked increase (generations 12 to 16) of collapsibility of peripheral airways;

Case B: markedly increased collapsibility of the peripheral airways (generations 8 to 16) with moderate involvement of the central ones (generations 4 to 7);

Case C: markedly increased collapsibility of both central and peripheral airways (generations 4 to 16)

Case D: markedly increased collapsibility of the central airways (generations 4 and 5) with moderate involvement of the remaining airways (generations 6 to 16);

Expiratory flow limitation was evaluated from isovolume pressure-flow curves computed at two lung volumes above the equilibrium volume. These curves were obtained following the procedure described by Lourens et al. (2001): a set of resistances was added to the outlet of the expiratory valve of the ventilator, thus producing expirations with different driving pressures, i.e. alveolar minus tracheal pressure. To quantify the extent of EFL, the negative expiratory pressure method was used to assess the fraction of the tidal volume for which the expiratory flow was the same with and without the negative expiratory pressure (Valta et al, 1994): the pressure at the outlet of the expiratory valve was set at of –5 cmH_2O throughout the test expiration, and the expiratory flow with the negative expiratory pressure was considered greater than that of control expiration at the same volume if the difference exceeded 3% of the peak expiratory flow of control expiration.

The interrupter flow resistance (R_{INT}) of the model's tracheobronchial tree was computed from the immediate changes of tracheal pressure with the insertion of an end-inflation pause, according to the rapid, end-inspiratory occlusion technique (Bates et al, 1985).

3. Results

During air and heliox ventilation, R_{INT} of the normal lung model was 1.5 and 1.05 $cmH_2O \cdot s \cdot l^{-1}$, respectively. Corresponding values for case A to D are shown in Table 2. During air breathing, R_{INT} was the least with the involvement of only the most peripheral airways (case A), and the highest when the alterations of the central airways were the greatest (D). On heliox, R_{INT} was nearly the same with all types of airway mechanical alterations, owing to the reduced impact of turbulence.

Fig. 2,left shows the isovolume pressure-flow curves obtained under the various conditions during air breathing at volumes 0.75 and 0.55 l above the equilibrium volume. The asterisk indicates the situation pertaining to control expirations, i.e. without external resistance or NEP application. Since with changing the driving pressure around the control value the expiratory flow either remained unchanged or even decreased, severe EFL was present in all cases and, as a consequence, dynamic hyperinflation developed. The latter was quantified by ΔFRC and PEEPi, the values of these variables being reported in Table 2.

Fig. 3 shows the flow-volume curves during a control expiration and one with NEP for a normal and diseased lung (case A) while breathing air. As expected, under normal conditions the expiratory flow increased markedly with negative expiratory pressure, and the flow limited portion of the expired tidal volume (FLP) is nil. On the contrary, application of negative expiratory pressure in case A did not change expiratory flow with respect to the control breath, except at the beginning of expiration, and FLP=87.4%. Similar results were obtained in the other cases, as shown by the corresponding FLP values (Table 2). In spite of similar FLP values, the sites of equal pressure point during a tidal expiration, i.e. the point where pleural pressure equals lateral pressure inside the bronchial tree, differed substantially among the various conditions, because of the differences in the $d_b\%{-}P$ curves of the affected airway generations. Thus: 1) in case A, the equal pressure point moved rapidly to generation 9, and reached generation 11 slightly before 50% VT was expired; 2) in case B, the equal pressure point moved rapidly to generation 4, and reached generation 5 and 7 when ~ 65 and 80% VT was expired; 3) in case C, the equal pressure point stayed within generation 3 until ~80% VT was expired, moving thereafter to generation 4; and 4) in case D, the equal pressure point remained within generation 3 during the entire expiration.

Fig. 2,right shows the isovolume pressure-flow curves obtained under the various conditions during heliox breathing at volumes 0.75 and 0.55 l above the equilibrium volume. In no case did heliox avoid EFL, change the location of the equal pressure point during expiration, and reduce FLP appreciably with respect to air ventilation (Table 2). On the other hand, relative to air ventilation, a decrease of ΔFRC and PEEPi occurred with heliox in cases C and D, but not in case A and B (Table

2). This different response is illustrated in Fig. 4, which shows the expiratory flow-volume curves of control breaths obtained in case A to D during air or heliox ventilation. With identical ventilator settings, no change in expiratory flow occurred between air and heliox in case A, except for an increase in the initial flow spike, which was mainly due to the effect of the lower gas density on equipment resistance. In case B, expiratory flow increased with heliox over most of the VT, the flow-volume curves with air and heliox superimposing only for the final 25% VT. Nevertheless, the change of ΔFRC with heliox was trivial in case B (31 ml or 6% ΔFRC on air), as it was in case A (Table 2). On the contrary, owing to a substantial reduction of the turbulence, expiratory flow increased with heliox over the entire VT when the changes in the mechanical properties of the central airways were marked, thus leading to a decrease of the end-expiratory volume which was moderate in case C (80 ml or 23% ΔFRC on air) and substantial in case D (173 ml or 41% ΔFRC on air). The rightward and downward shift of the expiratory flow-volume curve with heliox was in fact greater in case D than C, showing that the reduction of the hyperinflation is strongly dependent on the entity of the mechanical alteration of the central airways, rather than of the concomitant changes in peripheral airway mechanics.

4. Discussion

4.1 Inspiratory effects of heliox

The geometrical and mechanical characteristics attributed to the present mathematical model of the human tracheobronchial tree satisfactorily reproduce the airway resistive properties of both normal subjects and severe COPD patients, this conclusion being reached on the basis of the comparison of inspiratory viscous resistances. Indeed, with similar ventilator settings and during air breathing, R_{INT} predicted by the model for the normal lung (1.5 $cmH_2O \cdot s \cdot l^{-1}$) was within the range of lung R_{INT} values (1.1-2.3 $cmH_2O \cdot s \cdot l^{-1}$) reported for normal, anaesthetised paralysed subjects (Jonson et al, 1993; D'Angelo et al, 1994), while R_{INT} values predicted by the model for abnormal lungs (Table 2) were close to those obtained in mechanically ventilated COPD patients (Broseghini et al, 1988; Guérin et al, 1993). Case A to D simulate, therefore, the condition of severe pulmonary obstruction, potentially necessitating mechanical ventilation.

As expected, R_{INT} decreased with heliox administration, except in case A when the increase in R_{INT} is entirely due to that of the resistance of the peripheral airways, where flow is predominantly laminar. With an inspiratory flow of ~1 $l \cdot s^{-1}$, R_{INT} decreased by about 20 and 30% in case B-C and D, respectively (Table 2). Hence, the inspiratory resistive work is reduced with heliox breathing, a fall that can be appreciable, depending on the inspiratory flow. In this respect, obstructed patients should benefit from heliox administration, in line with clinical observations.

4.2 Expiratory effects of heliox

The beneficial effects of heliox administration on expiration are reduction of dynamic hyperinflation and PEEPi. In the absence of EFL, dynamic hyperinflation can ensue only because of excessive shortening of expiratory duration relative to the expiratory effort. As turbulent flow likely develops, heliox administration would results in a decrease of dynamic hyperinflation at fixed expiratory duration and effort, and to an extent predictable from R_{INT} values. In the presence of EFL, no prediction can be made of the expiratory effects of heliox administration from the concomitant R_{INT} changes, but they can be understood through the analysis of the behaviour of airways resistance, as it determines expiratory flow. Due to dynamic hyperinflation, pleural pressure (p_{pl}) can reach high values in flow limited patients; because of the pressure drop along the airways during expiration, p_{pl} eventually compresses the airways downstream of the equal pressure point and airway resistance markedly exceeds that during inspiration (Avanzolini et al, 2001). Under these conditions, flow is driven by the difference between alveolar pressure (p_{alv}) and p_{pl} (Starling resistor effect): the total apparent airway resistance is given by

$$R_{APP} = \frac{p_{alv} - p_{pl}}{q} \tag{3}$$

while the apparent resistance of the peripheral airways, i.e. that upstream of generation 7, is

$$R_{PAW} = \frac{p_{alv} - p_{8th}}{q} \tag{4}$$

p_{8th} representing intraluminal pressure of generation 8. The expiratory time course of R_{APP} and R_{PAW} that occurred in the model under the various conditions during air and heliox ventilation is shown in Fig. 5. While R_{APP} was essentially the same on air and heliox in case A and B, it decreased markedly with heliox throughout expiration in case C and D, leading to an appreciable reduction of dynamic hyperinflation, as indicated by ΔFRC and PEEPi changes (Table 2).

The analysis of the expiratory time course of R_{APP} and R_{PAW} under the various conditions helps to elucidate the mechanisms underlying the different responses to heliox administration. Furthermore, it can be performed in the anaesthetised subject, when all parameters in Eqs. (3) and (4) become measurable. With severe obstruction of deep airways as in case A, R_{PAW} was greater than R_{APP}, except during the rapid initial flow spike, showing that the equal pressure point is located in peripheral airways during nearly the entire expiration. Consequently, the turbulent component of R_{APP} is negligible, EFL is due to the viscous mechanism, and no improvement of dynamic hyperinflation can be expected from heliox administration. In case B, R_{APP} exceeded R_{PAW} during

most of expiration, but R_{PAW} rose above R_{APP} before the end of expiration, showing that the equal pressure point eventually reaches the peripheral airways. Consequently, the flow during the final part of expiration is again limited by the viscous mechanism, and, hence, ΔFRC and PEEPi cannot decrease appreciably with heliox administration. In contrast, R_{APP} exceeded R_{PAW} throughout the whole expiration both during air and heliox ventilation in case C and D, showing that the equal pressure point is always located in the central airways, EFL is due to the wave-speed mechanisms, and an improvement of dynamic hyperinflation must be expected from heliox administration.

The comparison of R_{APP} and R_{PAW} time course of case B and C highlights the importance of the relative entity of the mechanical alterations of peripheral and central airways in determining the beneficial effects of heliox administration on dynamic hyperinflation. Indeed, in both cases heliox actually increased R_{PAW}, particularly towards the end of expiration, because the Poiseuille term of the resistance is predominant in lower conductive airways and the greater viscous pressure loss with heliox led to a decreased airway diameter relative to air ventilation. In case C, however, the increase of R_{PAW} with heliox was overcompensated by the concomitant decrease in the resistance of the central airways. In fact, turbulent flow developed in these airways, owing to their marked narrowing. As a consequence, heliox administration allowed for a decrease of R_{APP}, an increased flow during the entire expiration, and a reduction of dynamic hyperinflation. On the contrary, in case B turbulence in the central airways developed only during the initial part of expiration, as airway diameter of generations 4 to 7 were substantially greater than in case C, and R_{APP} could decrease appreciably with heliox only during that part of expiration, thus allowing for a small increase of mean expiratory flow and reduction of dynamic hyperinflation. The different effectiveness of heliox administration in case D and C can also be explained along the same lines. Although in both cases the changes in the mechanical characteristics of the central airways were the same and the equal pressure point remained in the segmental bronchi for the entire expiration, the contribution of R_{PAW} to R_{APP} was negligible only in case D, whereby the decreased turbulence with heliox could lead to higher expiratory flows and larger decrease in ΔFRC and PEEPi (Table 2).

4.3 Model based interpretation of clinical observations

The results of this model analysis indicate that in the presence of EFL the reduction of dynamic hyperinflation with heliox administration is trivial (case A and B), even when the contribution of the viscous mechanism to EFL becomes preponderant only during the final part of expiration. Also in case C, when the additional involvement of central airways was marked and flow limitation due to the wave-speed mechanism, the reduction of ΔFRC and PEEPi with heliox is modest, because the contribution of peripheral to total apparent airway resistance remains elevated.

Moreover, it should be noticed that the reductions of ΔFRC and PEEPi with heliox reported in Table 2 are the largest that can possibly occur under the specified conditions, since EFL was never abolished by heliox. A substantial improvement of dynamic hyperinflation with heliox occurred, therefore, in case D only, when EFL is still due to the wave-speed mechanism, but the contribution of peripheral airway to total apparent resistance is marginal. It is generally maintained that COPD affects primarily the peripheral airways, especially the small ones. In this perspective, case A to C can be regarded as subsequent stages of typical COPD, which, originating in the most peripheral airways, eventually involves the whole intrapulmonary bronchial tree, while case D could represent severe asthma with mild involvement of peripheral airways or, conversely, mild COPD with a marked involvement of central airways. Hence, to the extent that the same mechanisms operating in the model are responsible for the occurrence of EFL in COPD patients, heliox administration should not be expected to appreciably reduce dynamic hyperinflation in the majority of COPD patients who are flow-limited at rest.

This conclusion is supported by the results of a recent study showing permanence of EFL and absence of changes in the inspiratory capacity with heliox administration in a group of eighteen COPD patients who were flow limited while breathing air at rest (Pecchiari et al, 2004). There is only a limited number of studies in COPD patients, either mechanically ventilated or spontaneously breathing at rest, in which the effects of heliox administration on dynamic hyperinflation have been assessed; some of them have reported a substantial reduction of ΔFRC or PEEPi with heliox relative to air breathing (Swidwa et al, 1985; Gainnier et al, 2003; Jolliet et al, 2003; Lee et al, 2005), whilst others have failed to observe any appreciable change (Grapé et al, 1960; Jaber et al, 2000; Diehl et al, 2003; Palange et al, 2004). According to the results of the present model analysis, this discrepancy could reflect the different frequency with which the disease involved the peripheral and the central airways in the various groups of COPD patients, but in these studies the presence of EFL was not assessed, whereas it always occurred in the present simulations.

Interestingly, in none of the present conditions did heliox administration affect EFL, since FLP remained essentially the same even when the fall in ΔFRC and PEEPi was appreciable, as in case D and, to a lesser extent, case C (Table 2), possibly because the fall of R_{APP} was too small to prevent EFL (Fig. 5), while the concomitant compression of peripheral airways enhanced the impact of the viscous mechanism. This observation would in fact indicate that during spontaneous breathing and in the presence of EFL, no further amelioration of dynamic hyperinflation can be obtained with heliox administration by increasing the expiratory effort, or augmentation of pulmonary ventilation at fixed expiratory effort by shortening expiratory duration, as dynamic hyperinflation would increase. It must be, however, pointed out that the observation above might

not have general validity, as it has been made in a limited number of cases, though representative of a variety of airway alterations causing marked dynamic hyperinflation and EFL during air breathing at rest. Further simulation tests should be, therefore, performed in order to assess whether the inability of heliox to eliminate EFL is the rule, as well as to ascertain the impact of the magnitude of the changes of airway properties on the effectiveness of heliox administration in reducing both dynamic hyperinflation and, possibly, EFL.

Secretions, by reducing the effective airway caliber at any given transmural pressure, could eventually cause flow limitation in the bronchial area involved. The presence of flow limited compartments in parallel with non flow limited ones implies that this flow limitation cannot be detected by measurements performed at the airway opening. Actually, under this condition there is no tidal EFL, according to its definition, because the expiratory flow remains effort dependent. Given their random occurrence, it is seems highly unlikely that secretions can effectively involve all the airways of a peripheral generation, while this might be more plausible for the central airways, *e.g.* the 4^{th} and 5^{th} generation, thus reproducing the conditions of case D. Heliox administration should then reduce the dynamic hyperinflation caused by tidal EFL.

In the present simulation, tidal volume and breathing frequency were kept the same during ventilation on air and heliox, as neither parameter does change with heliox in spontaneously breathing COPD patients at rest (Grapé et al, 1960; Bradley et al, 1980; Swidwa et al, 1985; Jaber et al, 2000; Gainnier et al, 2003; Jolliet et al, 2003; Diehl et al, 2003; O'Donoghue et al, 2004; Palange et al, 2004; Lee et al, 2005; Eves et al, 2006), independent of the presence of EFL (Pecchiari et al, 2004). On the other hand, because of the fall in R_{INT} with heliox (Table 2), at fixed tidal volume and breathing frequency, the inspiratory duration should shorten and the expiratory duration lengthen, thus allowing for an appreciable fall in case B-C and a further reduction in case D of ΔFRC and PEEPi. Moreover, the fall of PEEPi would lead to a decreased inspiratory elastic work, reduced inspiratory effort at fixed tidal volume, and improved respiratory sensation. There are only a few reports concerned with the effects of heliox on breath timing in COPD patients at rest; except one study in patients during pressure support ventilation showing a 0.4 s decrease of inspiratory duration and increase of expiratory duration with heliox (Jolliet et al, 2004), all other reports indicate that in moderate or severe COPD patients heliox has no effect on breath timing (Bradley et al, 1980; Swidwa et al, 1985; Jaber et al, 2000; Diehl et al, 2003; Pecchiari et al, 2004; O'Donoghue et al, 2004; Eves et al, 2006), thus suggesting that during resting ventilation the control system readjust respiratory muscle activity, keeping tidal volume, respiratory rate, and breath timing fixed. As a consequence, the effects of heliox on dynamic hyperinflation predicted by

the present simulations during mechanical ventilation are likely to be seen also during quiet breathing in flow-limited COPD patients.

In conclusion, the present model study suggests that in severe COPD patients with EFL, reduction of dynamic hyperinflation with heliox administration during resting breathing should be trivial when the alterations are limited to the peripheral airways, whereas with the involvement of central airways a substantial decrease of dynamic hyperinflation should occur only if the concomitant changes of peripheral airway mechanics were minor. This explains, at least in part, the conflicting reports concerned with the expiratory effects of heliox administration in COPD patients during resting breathing or mechanical ventilation. While pointing to the need of assessing the mechanisms causing EFL to understand the effects of heliox administration, this study also show how those mechanisms can be recognised through the analysis of peripheral and total apparent resistance, which is feasible in anaesthetised subjects. Finally, the results indicate that heliox administration should not modify the extent of EFL, independent of whether EFL is due to the wave-speed or viscous mechanism, thus preventing the possibility that dynamic hyperinflation can be reduced by increasing the driving pressure.

References

Avanzolini, G., Barbini, P., Bernardi, F., Cevenini, G., Gnudi, G., 2001. Role of the mechanical properties of tracheobronchial airways in determining the respiratory resistance time course. Ann. Biomed. Eng. 29: 575-586.

Barach, A., 1935. The use of helium in the treatment of asthma and obstructive lesions in the larynx and trachea. Ann. Intern. Med. 9: 739-765.

Barbini, P., Brighenti, C., Cevenini, G., Gnudi, G., 2005. A dynamic morphometric model of the normal lung for studying expiratory flow limitation in mechanical ventilation. Ann. Biomed. Eng. 33: 518–530.

Bates, J.H., Rossi, A., Milic-Emili, J., 1985. Analysis of the behaviour of the respiratory system with constant inspiratory flow. J. Appl. Physiol. 58: 1840-1848.

Bradley, B.L., Forman, J.W., Miller, W.C., 1980. Low-density gas breathing during exercise in chronic obstructive lung disease. Respiration 40: 311-316.

Broseghini, C., Brandolese, R., Poggi, R., Polese, G., Manzin, E., Milic-Emili, J., Rossi, A., 1988. Respiratory mechanics during the first day of mechanical ventilation in patients with pulmonary edema and chronic airway obstruction. Am. Rev. Respir. Dis. 138: 355-361.

Chevrolet, J.C., 2001. Helium oxygen mixtures in the intensive care unit. Critical Care 5: 179-181.

D'Angelo, E., Prandi, E., Tavola, M., Calderini, E., Milic-Emili, J., 1994. Chest wall interrupter resistance in anesthetized paralyzed humans. J. Appl. Physiol. 77: 883-887.

Diehl, J.L., Mercat, A., Guerot, E., Aïssa, F., Teboul, J.L., Richard. C., Labrousse, J., 2003. Helium/oxygen mixture reduces the work of breathing at the end of the weaning process in patients with severe chronic obstructive pulmonary disease. Crit. Care Med. 31: 1415-1420.

Eves, N.D., Petersen, S.R., Haykowsky, M.J., Wong, E.Y., Jones, R.L., 2006. Helium-hyperoxia, exercise, and respiratory mechanics in chronic obstructive pulmonary disease. Am. J. Respir. Crit. Care Med. 174: 763-771.

Gainnier, M., Arnal, J.M., Gerbeaux, P., Donati, S., Papazian, L., Sainty J.M., 2003. Helium-oxygen reduces work of breathing in mechanically ventilated patients with chronic obstructive pulmonary disease. Int. Care Med. 29: 1666-1670.

Gerbeaux, P., Gainnier, M., Arnal, J.M., Papazian, L., Jean, P., Sainty, J.M., 2005. Effects of helium–oxygen mixtures on endotracheal tubes: an in vitro study. J. Biomech. 38: 33-37.

Grapé, B., Channin, E., Tyler, J.M., 1960. The effect of helium and oxygen mixtures on pulmonary resistances in emphysema. Am. Rev. Respir. Dis. 81: 823-829.

Guérin, C., Coussa, M.L., Eissa, N.T., Corbeil, C., Chassé, M., Braidy, J., Matar, N., Milic-Emili, J., 1993. Lung and chest wall mechanics in mechanically ventilated COPD patients. J. Appl. Physiol. 74: 1571-1580.

Ho, A.M.H., Lee, A., Karmakar, M.K., Dion, P.W., Chung, D.C., Contardi, L.A.H., 2003. Heliox vs air-oxygen mixtures for the treatment of patients with acute asthma. Chest 123: 882-890.

Hyatt, R.E., 1983. Expiratory flow limitation. J. Appl. Physiol. 55:1-7.

Jaber, S., Fodil, R., Carlucci, A., Boussarsar, M., Pigeot, J., Lemaire, F., Harf, A., Lofaso, F., Isabey, D., Brochard, L., 2000. Noninvasive ventilation with helium-oxygen in acute exacerbations of chronic obstructive pulmonary disease. Am. J. Respir. Crit. Care Med. 161: 1191-1200.

Jolliet, P., Watremez, C., Roeseler, J., Ngengiyumva, J.C., de Kock, M., Clerbaux, T., Tassaux, D., Reynaert, M., Detry, B., Liistro, G., 2003. Comparative effects of helium-oxygen and external positive end-expiratory pressure on respiratory mechanics, gas exchange, and ventilation-perfusion relationships in mechanically ventilated patients with chronic obstructive pulmonary disease. Int. Care Med. 29: 1442-1450.

Jonson, B., Beydon, L., Brauer, K., Manson, C., Valid, S., Grytzell, H., 1993. Mechanics of respiratory system in healthy anesthetized humans with emphasis on viscoelastic properties. J. Appl. Physiol. 75: 132-140.

Lambert, R.K., 1989. A new computational model for expiratory flow from nonhomogeneous human lungs. J. Biomech. Eng. 111:200-205.

Lee, D.L., Lee, H., Chang, H.W., Chang, A.Y., Lin, S.L., Huang, Y.C.T., 2005. Heliox improves hemodynamics in mechanically ventilated patients with chronic obstructive pulmonary disease with systolic pressure variations. Crit. Care Med. 33: 968-973.

Lourens, M.S., Berg, B.V.D., Verbraak, A.F.M., Hoogsteden, H.C., Bogaard, J.M., 2001. Effect of series of resistance levels on flow limitation in mechanically ventilated COPD patients. Respir. Physiol. 127: 39-52.

Manthous, C.A., Morgan, S., Pohlman, A., Hall J.B., 1997. Heliox in the treatment of airflow obstruction: a critical review of the literature. Respiratory Care 42: 1034-1042.

Marini, J.J., 2000. Heliox in chronic obstructive pulmonary disease: time to lighten up? Crit. Care Med. 28: 3086-3088.

O'Donoghue, F.J., Catcheside, P.G., Eckert, D.J., McEvoy, R.D., 2004. Changes in respiration in NREM sleep in hypercapnic chronic obstructive pulmonary disease. J Physiol. 559: 663-673.

Palange, P., Valli, G., Onorati, P., Antonucci, R., Paoletti, P., Rosato, A., Manfredi, F., Serra, P., 2004. Effect of heliox on lung dynamic hyperinflation, dyspnea, and exercise endurance capacity in COPD patients. J. Appl. Physiol. 97: 1637-1642.

Papamoschou, D., 1995. Theoretical validation of the respiratory benefits of helium-oxygen mixtures. Respir. Physiol. 99: 183-199.

Pecchiari, M., Pelucchi, A., D'Angelo, E., Foresi, A., Milic-Emili, J,, D'Angelo, E., 2004. Effect of heliox breathing on dynamic hyperinflation in COPD patients. Chest 125: 2075-2082.

Pedley, T.J., Schroter, R.C., Sudlow, M.F., 1970. The prediction of pressure drop and variation of resistance within the human bronchial airways. Respir. Physiol. 9:387-405.

Rodrigo, G., Pollack, C., Rodrigo, C., Rowe, B., 2002. Heliox for treatment of exacerbations of chronic obstructive pulmonary disease. Cochrane Database Syst. Rev. CD003571.

Tassaux, D., Jolliet, P., Roeseler, J., Chevrolet, J.C., 2000. Effects of helium-oxygen on intrinsic positive end-expiratory pressure in intubated and mechanically ventilated patients with severe chronic obstructive pulmonary disease. Crit. Care Med. 28: 2721-2728.

Swidwa, D.M., Montenegro, H.D., Goldman, M.D., Lutchen, K.R., Saidel, G.M., 1985. Helium-oxygen breathing in severe chronic obstructive pulmonary disease. Chest 87: 790-795.

Valta, P., Corbeil, C., Lavoie, A., Campodonico, R., Koulouris, N., Chasse, M., Braidy, J., Milic-Emili, J., 1994. Detection of expiratory flow limitation during mechanical ventilation. Am. J. Respir. Crit. Care Med. 150:1311-1317.

Weibel, E.R., 1963. Morphometry of the human lung. Springer-Verlag, Berlin.

West, J.B., 1998. Pulmonary Pathophysiology-The essential, 5th ed., Williams & Wilkins, Baltimore.

Wouters, E.F.M., Landser, F.J., Polko, A.H., Visser, B.F., 1992. Impedance measurement during air and helium-oxygen breathing before and after salbutamol. Clin. Exper. Pharm. Physiol. 19:95-101.

Legends

Fig. 1. The relationships between transmural pressure and branch diameter, expressed as percent of maximum, in case A to D. The numbers indicate branch generation.

Fig. 2. Isovolume pressure-flow curves in case A to D during air (left) and heliox (right) ventilation obtaining for lung volumes 750 (upper lines) and 550 ml above the equilibrium volume. The asterisks correspond to control expiration.

Fig. 3. Expiratory flow-volume curves of the control breath and one with application of negative expiratory pressure (continuous and dashed line, respectively) for the normal lung and case A. Lung volume (ΔV) is expressed as difference from equilibrium volume.

Fig. 4. Expiratory flow-volume curves of control breaths during air and heliox ventilation (continuous and dashed line, respectively) in case A to D. Lung volume (ΔV) is expressed as difference from equilibrium volume.

Fig. 5. Expiratory time course of peripheral and total apparent resistance (bold and thin lines, respectively) during air and heliox ventilation (continuous and dashed line, respectively) in case A to D. For definition of peripheral and total apparent resistance see text (Eqs. 3 and 4).

Table 1 – Branch length (l_b) and diameter (d_b), and parameters in Eqs. 1 and 2 for normal lungs

Generation	$d_b$max (mm)	l_b (mm)	k_b (Air) ($s \cdot l^{-1}$)	k_b (HeO_2) ($s \cdot l^{-1}$)	α_0	α'_0 (cmH_2O^{-1})	g
0	18.1	70.0	11.93	6.30	0.882	0.0294	10
1	12.3	47.6	10.03	5.21	0.882	0.0294	10
2	8.34	19.0	11.39	5.99	0.686	0.0500	10
3	5.63	7.6	12. 90	6.86	0.550	0.0784	10
4	4.52	12.7	6.43	3.13	0.495	0.0980	10
5	3.52	10.7	4.63	2.09	0.445	0.1225	10
6	2.81	9.0	3.26	1.29	0.410	0.1392	10
7	2.31	7.6	2.19	0.68	0.385	0.1559	10
8	1.87	6.4	1.37	0.20	0.362	0.1706	10
9	1.55	5.4	0.73	0	0.346	0.1804	10
10	1.31	4.6	0.24	0	0.334	0.1902	10
11	1.10	3.9	0	0	0.324	0.2020	9
12	0.95	3.3	0	0	0.317	0.2137	8
13	0.82	2.7	0	0	0.310	0.2216	8
14	0.74	2.3	0	0	0.306	0.2284	8
15	0.66	2.0	0	0	0.302	0.2343	7
16	0.60	1.65	0	0	0.299	0.2382	7

For the trachea, l_b is the part free from endotracheal tube.

Table 2 – Interrupter flow resistance (R_{INT}), change in functional residual capacity (ΔFRC), intrinsic positive end-expiratory pressure (PEEPi), and flow limited portion of the tidal volume (FLP), expressed as a percentage of the expired volume, during air or heliox ventilation in case A to D

CASE	AIR				HELIOX			
	R_{INT} $cmH_2O \cdot s \cdot l^{-1}$	ΔFRC ml	PEEPi cmH_2O	FLP %	R_{INT} $cmH_2O \cdot s \cdot l^{-1}$	ΔFRC ml	PEEPi cmH_2O	FLP %
A	9.5	376	7.8	87.4	9.0	371	7.7	88.2
B	11.4	494	10.4	92.5	8.9	463	9.7	92.0
C	12.2	350	7.2	93.7	8.9	270	5.6	93.1
D	12.7	425	8.6	93.9	9.3	252	5.1	93.5

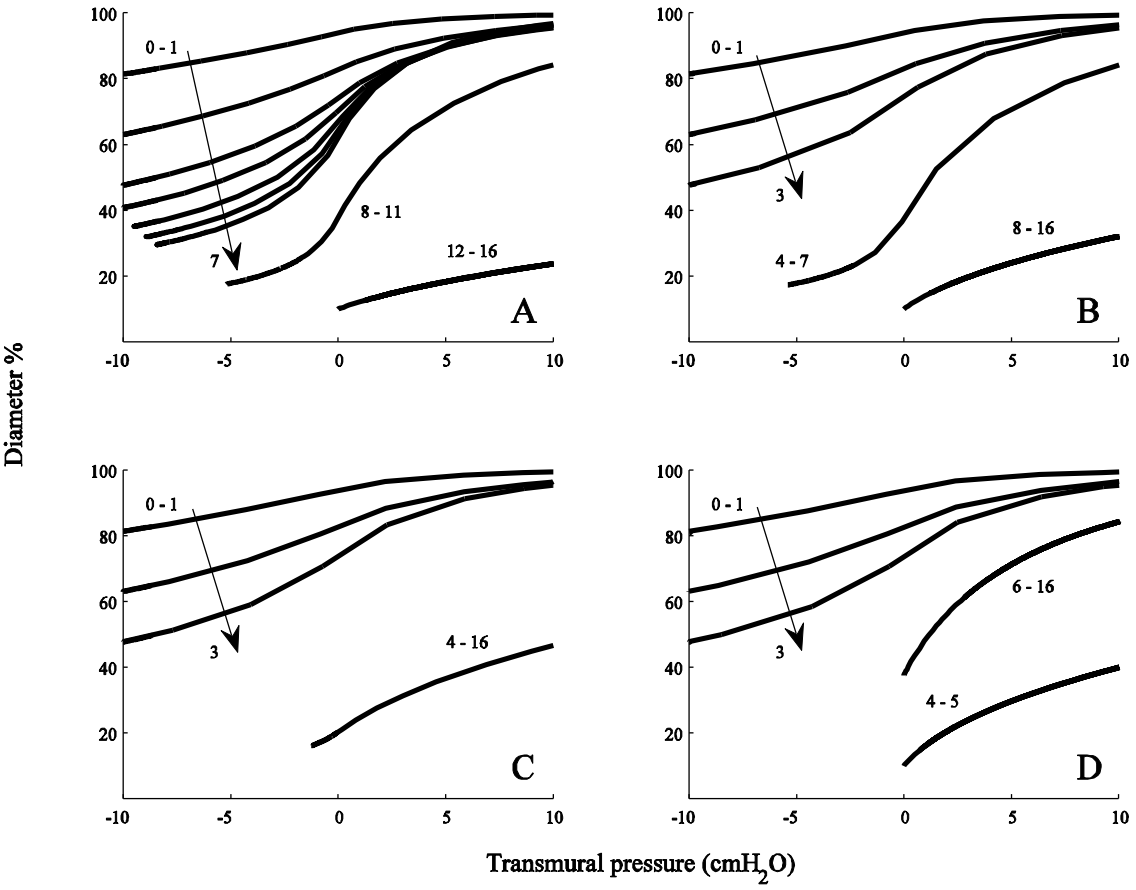
Diameter %
Transmural pressure (cmH2O)
A
B
C
D
0 - 1
7
8 - 11
12 - 16
3
4 - 7
8 - 16
4 - 16
6 - 16
4 - 5

Figure 1

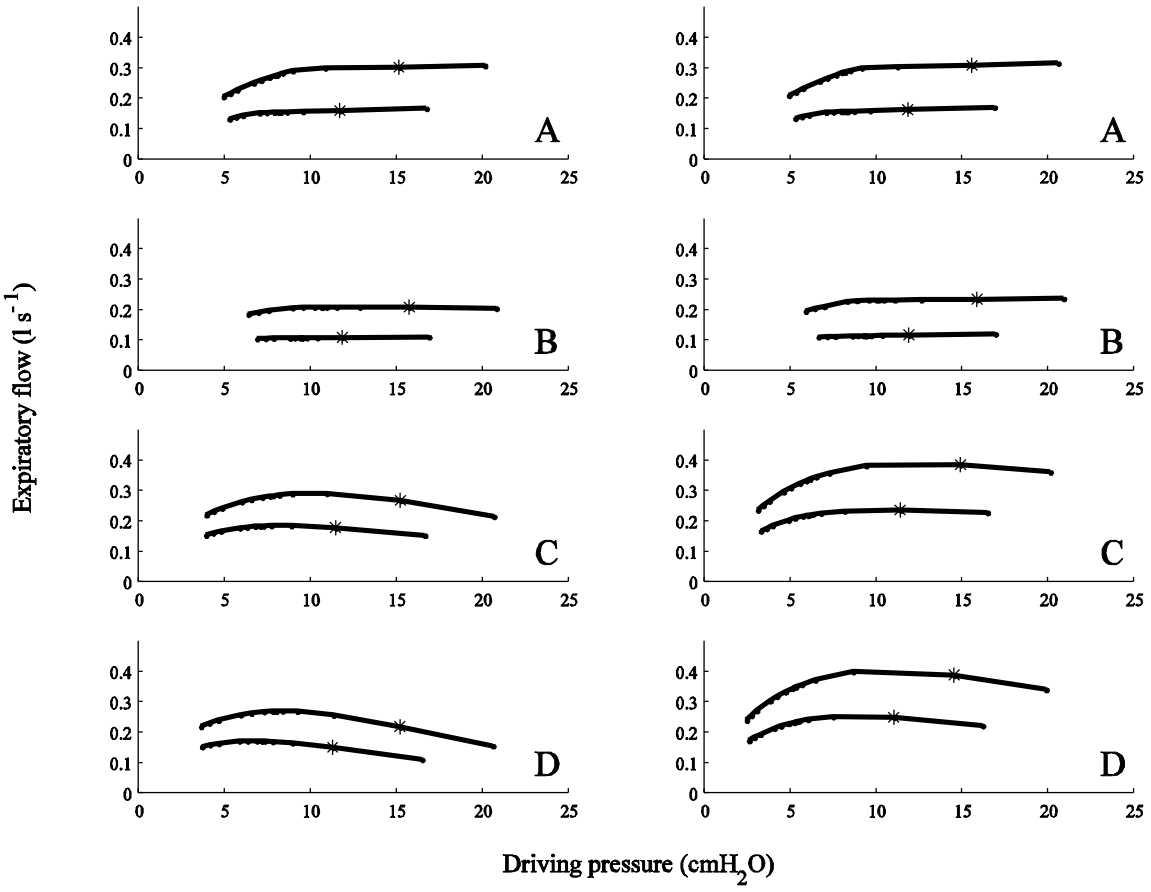

Figure 2

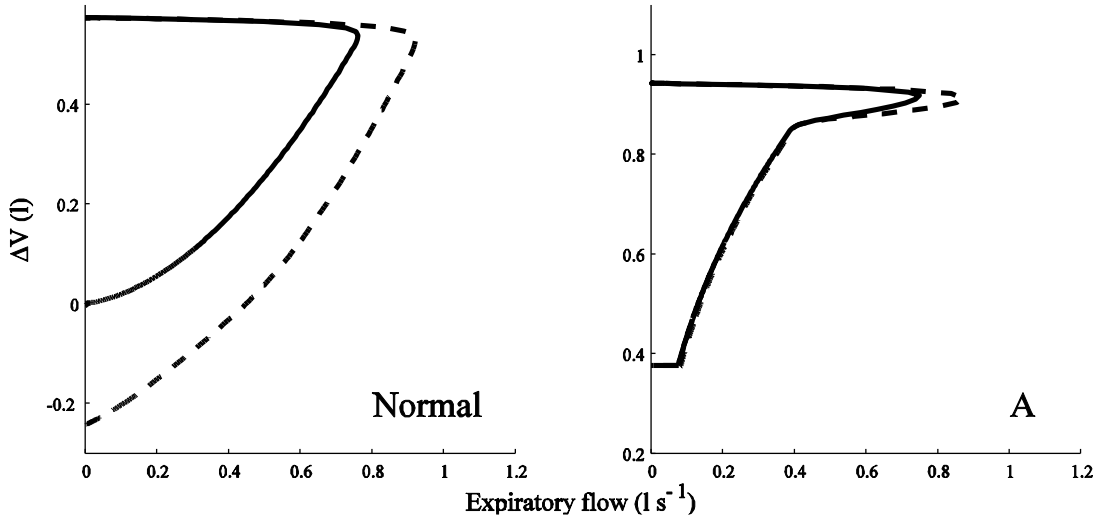
ΔV (l)
0.4
0.2
0
-0.2
Normal
0
0.2
0.4
0.6
0.8
1
1.2
1
0.8
0.6
0.4
0.2
A
Expiratory flow (l s-1)

Figure 3

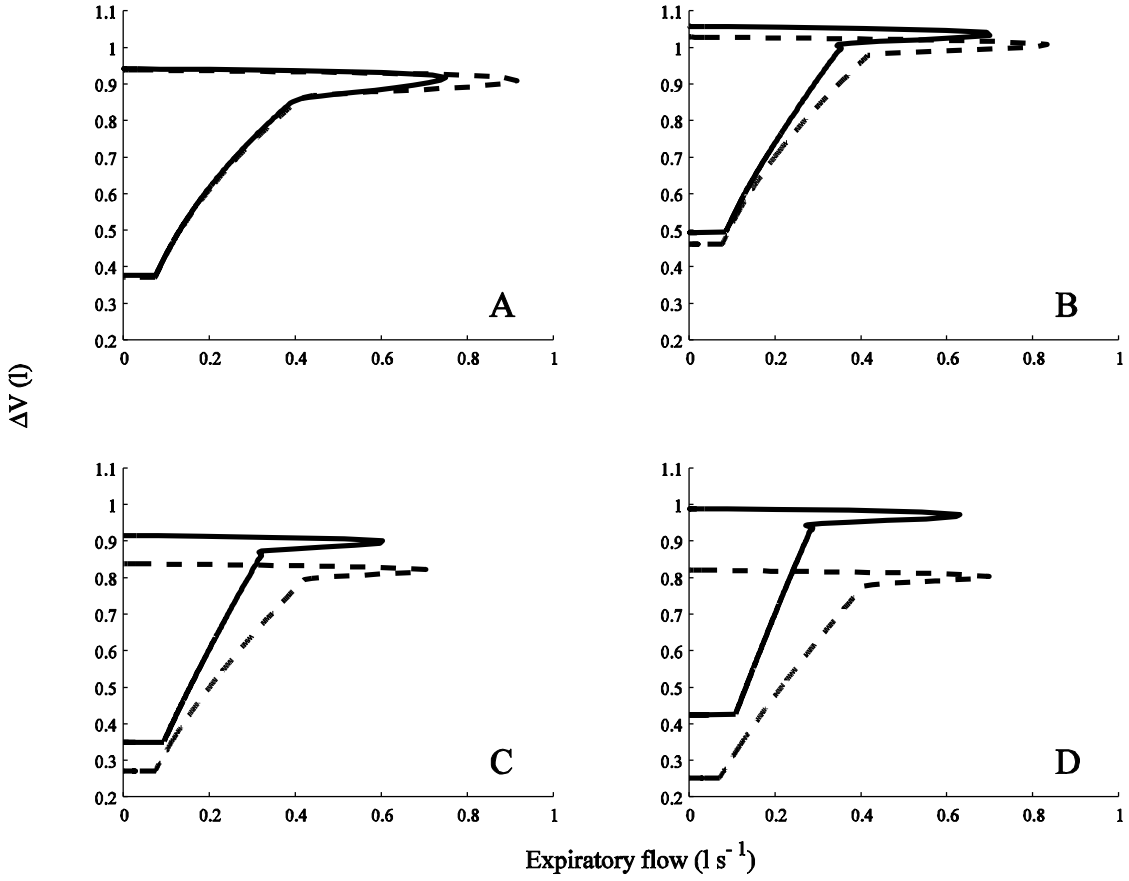

Figure 4

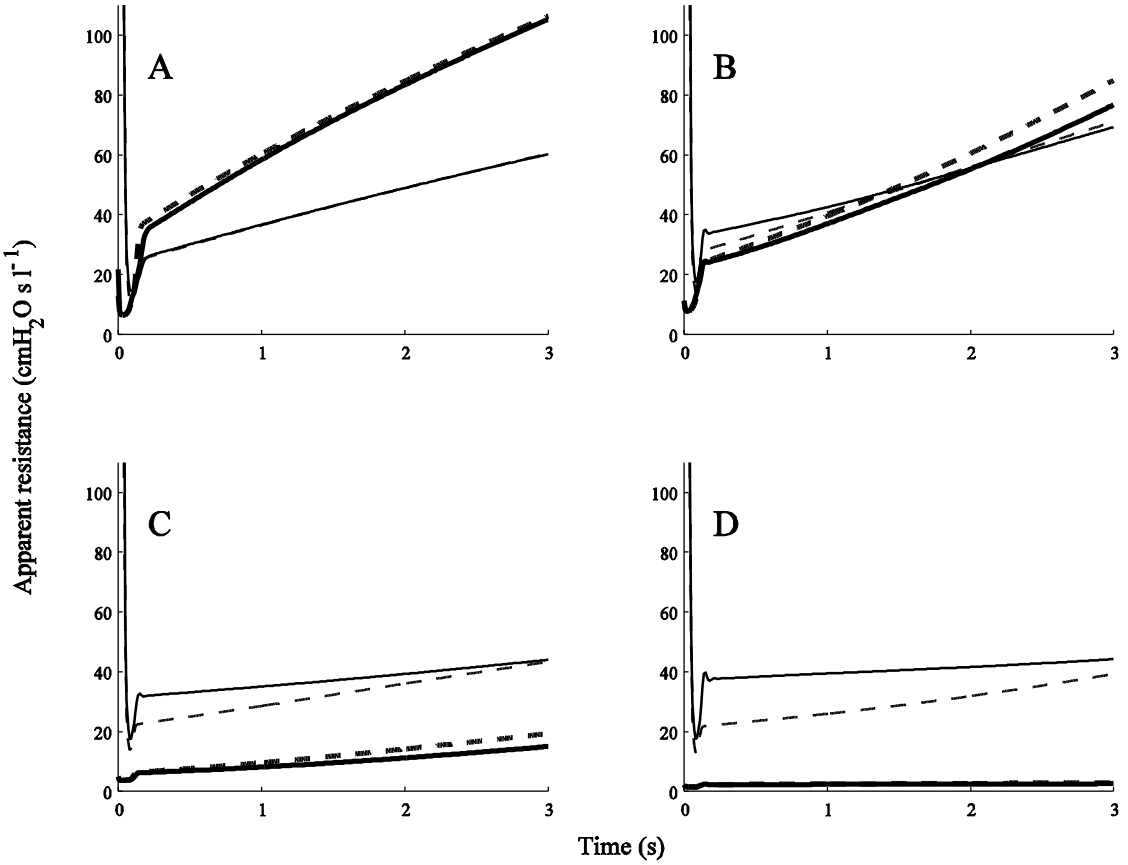
A
B
C
D
Apparent resistance (cmH2O s l-1)
Time (s)
0
20
40
60
80
100
0
1
2
3

Figure 5